Heliyon 10 (2024) e37278

Contents lists available at ScienceDirect

Heliyon

journal homepage: www.cell.com/heliyon

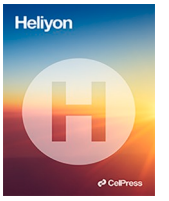

Research article

Inhibition of CTLA-4 accelerates atherosclerosis in hyperlipidemic mice by modulating the Th1/Th2 balance via the NF-κB signaling pathway

Ming-Luan Zhao [a,1], Chen Liang [a,b,1], Wei-Wei Jiang [a,1], Mei Zhang [a], Hong Guan [a], Zi Hong [a], Di Zhu [a], An-Qi Shang [a], Chang-Jiang Yu [b], Zhi-Ren Zhang [a,b,c,*]

[a] *Departments of Cardiology and Critical Care Medicine, The First Affiliated Hospital of Harbin Medical University (HMU), NHC Key Laboratory of Cell Transplantation, Key Laboratories of Education Ministry for Myocardial Ischemia Mechanism and Treatment, Harbin, 150001, China*
[b] *Departments of Cardiology and Pharmacy, HMU Cancer Hospital, Institute of Metabolic Disease, Heilongjiang Academy of Medical Science, Heilongjiang Key Laboratory for Metabolic Disorders and Cancer-related Cardiovascular Diseases, Harbin, 150081, China*
[c] *State Key Laboratory of Frigid Zone Cardiovascular Diseases (SKLFZCD), HMU, Harbin, 150081, China*

ARTICLE INFO

Keywords:
Anti-CTLA-4 antibody
Atherosclerosis
Th1/Th2 balance
NF-κB signaling pathway

ABSTRACT

Objective: Though an increased risk of atherosclerosis is associated with anti-CTLA-4 antibody therapy, the underlying mechanisms remain unclear.
Methods: C57BL/6 mice were treated with anti-cytotoxic T-lymphocyte-associated protein 4 (CTLA-4) antibody twice a week for 4 weeks, after being injected with AAV8-PCSK9 and fed a Paigen diet (PD). The proportion of aortic plaque and lipid accumulation were assessed using Oil Red O staining, while the morphology of atherosclerotic lesions was analyzed with hematoxylin and eosin staining. Collagen content was evaluated through Picrosirius Red (PSR) staining, while inflammatory cell infiltration was examined with immunofluorescence staining. $CD4^+$ T cells secreting IFN-γ and IL-4, which represent Th1 and Th2 cells respectively, were detected by flow cytometry and real-time PCR. Protein levels of p-IκBα, IκBα, p-p65, and p65 were determined by Western blot.
Results: Inhibiting CTLA-4 exacerbated PD-induced plaque progression and promoted $CD4^+$ T cell infiltration in the aortic root. The anti-CTLA-4 antibody promoted $CD4^+$ T cell differentiation toward the Th1 type, as indicated by an increase in the Th1/Th2 ratio. Compared to the anti-IgG group, treatment with anti-CTLA-4 antibody significantly elevated the protein levels of p-IκBα and p-p65, as well as the mRNA levels of TNF-α, IL-6, ICAM-1, and VCAM-1. Inhibiting the NF-κB

Abbreviations: AAV8-PCSK9, adeno-associated virus-8-mediated overexpression of proprotein convertase subtilisin/kexin type 9; ASCVD, atherosclerotic cardiovascular disease; CTLA-4, cytotoxic T-lymphocyte-associated protein 4; DEGs, differentially expressed genes; ESs, enrichment scores; GO, Gene Ontology; GSEA, gene set enrichment analysis; HDL-C, high-density lipoprotein cholesterol; H&E, hematoxylin and eosin; ICIs, Immune checkpoint inhibitors; KEGG, Kyoto Encyclopedia of Genes and Genomes; LDL-C, low-density lipoprotein cholesterol; MMPs, matrix metalloproteinases; NES, normalized enrichment score; ORO, oil red O; PBMCs, peripheral blood mononuclear cells; PCR, polymerase chain reaction; PD, Paigen diet; PD-1, programmed cell death protein 1; PD-L1, programmed death-ligand 1; PSR, Picrosirius Red; TC, cholesterol; Teffs, effector T cells; TG, triglyceride; WT, wild-type; α-SMA, α-smooth muscle actin.

* Corresponding author. Departments of Cardiology and Critical Care Medicine, NHC Key Laboratory of Cell Transplantation, The First Affiliated Hospital of Harbin Medical University 23 Youzheng Road, Harbin, 150081, China.
E-mail addresses: zhirenz@hrbmu.edu.cn, zhirenz@163.com (Z.-R. Zhang).
[1] These authors contributed equally to this work.

https://doi.org/10.1016/j.heliyon.2024.e37278
Received 10 March 2024; Received in revised form 28 August 2024; Accepted 30 August 2024
Available online 31 August 2024

signaling pathway attenuated the overall pathological phenotype induced by the anti-CTLA-4 antibody treatment.
Conclusion: Anti-CTLA-4 treatment promotes the progression of atherosclerosis by activating NF-κB signaling and modulating the Th1/Th2 balance. Our results provide a rationale for preventing and/or treating atherosclerosis accelerated by anti-CTLA-4 antibody therapy in cancer patients.

1. Introduction

Atherosclerosis is primarily driven by lipid deposition, which typically leads to plaque formation in large and medium-sized arteries [1,2]. Atherosclerosis is also a chronic inflammatory disease involving the immune system [3] and is a leading cause of death and disability worldwide [4–7]. Accumulated risk factors for atherosclerosis, including abnormal lipid metabolism, oxidative stress, decreased hydration, and inflammation, eventually lead to the disordered function of vascular cells and immune cells [8,9]. In the atherosclerotic inflammatory milieu, T cells are recruited by adhesion molecules and chemokines within lesions, where they produce proatherogenic mediators and initiate a cascade of inflammatory signaling pathways [10]. Immune checkpoint inhibitors (ICIs), such as programmed cell death protein 1 (PD-1), programmed death-ligand 1 (PD-L1), and cytotoxic T-lymphocyte-associated protein 4 (CTLA-4), are monoclonal antibodies that reinforce T-cell-mediated immune responses by blocking coinhibitory T-cell receptors and are approved for certain indications [11]. The potential for ICIs to accelerate the progression of atherosclerosis is strongly supported by clinical trials and animal models [12–15], and these immune checkpoints were shown to be critical negative regulators of atherosclerosis. The largest single-center study revealed that the use of ICIs was linked to an increase in the risk of composite cardiovascular events, myocardial infarction, coronary revascularization, and stroke [12]. Transgenic mice with constitutive CTLA-4 overexpression exhibited smaller atherosclerotic lesions at the aortic root and reduced infiltration of macrophages and $CD4^+$ T cells in plaques [14]. In addition, treatment with abatacept, a soluble CTLA-4 Ig fusion protein, reduced atherosclerosis in ApoE3-Leiden mice by preventing the activation of $CD4^+$ T cells [15]. Antibody-mediated inhibition of CTLA-4 accelerated the progression of atherosclerosis in $LDLr^{-/-}$ mice by inducing T-cell-driven inflammation and resulted in a 2-fold increase in the plaque area, larger necrotic cores and less collagen [13]. However, further studies are needed to identify the specific T-cell subtypes that are critical for the acceleration of atherosclerosis induced by anti-CTLA-4 antibody treatment.

Single-cell data from human atherosclerotic plaques and peripheral blood mononuclear cells (PBMCs) showed that the majority of $CD4^+$ T cells in the plaque were effector T cells (Teffs) [16]. The dominant Teffs in plaques were $CD4^+$ Th1 cells, which produce the cytokines IFN-γ, IL-12, and TNF-α. These cells activate macrophages and monocytes and increase the expression of matrix metalloproteinases (MMPs), resulting in thinning of the fibrous cap and an increased risk of plaque rupture [17,18]. Th2 cells, which are found in plaques in lower numbers, are considered protective, and the cytokine IL-4 they secrete produces complex effects [19]. It is commonly accepted that the classic Th1/Th2 paradigm is a key factor contributing to many inflammatory diseases, including atherosclerosis [20,21], asthma [22], and acute coronary syndrome [23,24]. Despite these previous studies, whether anti-CTLA-4 antibodies exacerbate atherosclerosis by regulating the Th1/Th2 ratio has not been fully elucidated.

Activation of the NF-κB signaling pathway plays a crucial role in the response to various external stimuli, such as inflammation, the immune response, cell proliferation, differentiation, and survival [25]. The transcription factor NF-κB has been associated with various inflammatory conditions, including atherosclerosis. NF-κB activation-mediated signaling has been observed at various points in the progression of atherosclerosis, from the formation of plaques to their destabilization and rupture [26]. Moreover, inhibition of the inflammatory activity of NF-κB could limit atherosclerotic plaque progression in mice [27]. In addition, several studies have described a role for NF-κB in Th1 cell differentiation. Th1 responses were significantly impaired due to a decrease in NF-κB activation in transgenic mice expressing a nondegradable form of IκB specifically in T cells [28]. However, the role of the NF-κB signaling pathway in atherosclerotic progression caused by anti-CTLA-4 antibodies is currently unknown.

In the present study, we showed that anti-CTLA-4 antibody treatment induced an imbalance in Th1 and Th2 cells, which was responsible at least in part for the anti-CTLA-4-mediated acceleration of T-cell activation and atherosclerosis in hyperlipidemic mice. Treatment with NF-κB inhibitors ameliorated anti-CTLA-4 antibody-induced atherosclerotic lesion formation and reversed the induction of T-cell differentiation to Th1 cells in adeno-associated virus-8-mediated overexpression of proprotein convertase subtilisin/kexin type 9 (AAV8-PCSK9) injected C57BL/6 mice fed a Paigen diet (PD). Gaining insight into the underlying mechanisms responsible for anti-CTLA-4 antibody-mediated promotion of atherosclerosis may facilitate the identification of specific therapeutic targets.

2. Material and methods

2.1. Animal models and experimental design

Male C57BL/6 mice (18–20 g) were purchased from Vital River Laboratory Animal Technology Co., Ltd. (Beijing, China) and bred at the Animal Centre of the Second Affiliated Hospital of Harbin Medical University. The mice were housed in sterilized filter-top cages and given free access to food and water with 12-h light/dark cycles.

To establish the atherosclerosis model, the six-week-old mice were injected with AAV8-PCSK9 (5×10^{11} viral particles/mL, WZ Biosciences, Inc.) via the tail vein and fed a sterilized PD containing 40 kcal% fat, 1.25 % cholesterol, and 0.5 % cholic acid (D12109C, Research Diets) for 16 weeks. After 12 weeks of feeding, the mice were randomly treated with the anti-CTLA-4 antibody (BE0032,

BioXcell) or an isotype control IgG2a antibody (BE0089, BioXcell) via intraperitoneal injection twice weekly for 4 consecutive weeks, as shown in Fig. S1A. Based on the doses reported in previous clinical trials and experiments conducted on mice, we administered a clinically relevant dose of 10 mg kg^{-1} of anti-mouse CTLA-4 antibody in this study [29–31].

For the NF-κB inhibitor experiment, after the induction of atherosclerosis at 12 weeks, hyperlipidemic mice were randomly injected with 0.1 mg/kg/d MG132 (474790, Sigma-Aldrich) for 4 consecutive weeks or 5 mg kg^{-1} BAY11-7082 (S2913, Selleck) three times per week for 4 weeks, as shown in Fig. S1A [32]. MG132 was dissolved in 0.2 % DMSO and diluted with saline for injection, and BAY11-7082 was dissolved in 10 % DMSO, 40 % PEG300, 5 % Tween 80, and 45 % ddH_2O for use.

2.2. Blood lipid index

Plasma total cholesterol (TC), triglyceride (TG), low-density lipoprotein cholesterol (LDL-C) and high-density lipoprotein cholesterol (HDL-C) levels were determined by commercial kits according to the manufacturer's instructions (Nan Jing Jian Cheng Biotech Co., Ltd.). Standard curves were created using the Curve Expert 1.3 software program.

2.3. Quantification of atherosclerosis

Mouse hearts were perfused with 10 mL of PBS. The whole aorta was dissected from the heart to the iliac bifurcation, and the adventitial tissue was carefully cleaned under a dissecting microscope. After fixation in 4 % paraformaldehyde (C104190, Aladdin) for 24 h, the aorta was dehydrated with 60 % isopropanol for 5 min, stained with 0.5 % Oil red O (ORO, O1391, Sigma-Aldrich) solution for 2 h and then destained in 70 % methanol for 5 min. The ORO area was quantified in sections using ImageJ software and reported as the lesion area.

Samples of the aortic root and coronary artery were preserved in OCT (4583, Sakura) and quickly frozen on dry ice. For Oil Red O staining, 8-μm-thick frozen sections were prepared and stained with freshly diluted Oil Red O staining solution for 10 min. After washed with 70 % ethanol, the sections were re-stained by Mayer hematoxylin for 4 min. The images were captured using a BX53 upright microscope (Olympus, Tokyo, Japan) and analyzed by Image J software.

2.4. Immunofluorescence analysis

Cryo-sections of the heart (8 μm thick) were subjected to immunofluorescence staining as previously described [33]. The slides were permeabilized with 0.2 % Triton X-100 for 10 min and washed with PBS containing 0.1 % (v/v) Tween 20 (PBS-T). After being blocked with 1 % BSA (4240, BioFroxx) for 30 min at room temperature (22-24 °C), the sections were incubated overnight at 4 °C with antibodies against CD4 (1:100, 14-9766-82, Thermo Fisher), anti-CD68 (1:100, 14-0681-82, Thermo Fisher), anti-IFN-γ antibody (1:100, PA5-95560, Invitrogen), anti-IL-4 polyclonal antibody (1:100, CSB-PA011659YA01HU, CUSABIO) and α-SMA (1:400, F3777, Sigma-Aldrich) diluted in PBS supplemented with 1 % BSA. The slides were incubated with Cy3-conjugated donkey anti-rat IgG (1:500, 712-166-153, Jackson ImmunoResearch) and Alexa Fluor 488-conjugated donkey anti-rabbit (1:500, 711-546-152, Jackson ImmunoResearch) for 1 h. The cell nuclei were counterstained with DAPI (1:1000, D1306, Invitrogen). The slides were imaged using a confocal microscope (Olympus Fluoview 1200, Japan). Quantitative analysis of sample images was performed using ImageJ software.

2.5. Histological analysis

The hearts were collected and perfused with 10 mL of PBS through the aortic arch puncture. They were fixed in 4 % paraformaldehyde for 48 h, dehydrated with graded ethanol and then subjected to paraffin embedding. Heart sections with a thickness of 3.5 μm were cut until the aortic root and coronary artery were located. These sections were deparaffinized in dimethylbenzene three times and subsequently rehydrated in 100 %, 95 %, 80 %, and 70 % ethanol, respectively. Hematoxylin-eosin (H&E) staining were performed according to the manufacturer's protocols of the H&E buffer (BA4027, Baso). For Picrosirius Red staining (PSR), deparaffinized sections were incubated in 0.2 % phosphomolybdic acid hydrate for 5 min, 0.1 % Sirius red solution (H26357, Head Biotechnology Co., Ltd.) for 60 min at room temperature and rinsed with hydrochloric acid (0.01 N) for 2 min. The slides were then mounted by coverslip using neutral gum (Biosharp, BL704A). The images were captured using a BX53 upright microscope (Olympus, Tokyo, Japan) and analyzed by Image J software. The plaque stability score was calculated as follows: (α-SMA-positive area + collagen-positive area)/(ORO area + CD68-positive area) [34,35].

2.6. Flow cytometry

One hundred microliters of mouse peripheral blood were collected in isotonic RPMI 1640 complete culture medium (R8758, Sigma-Aldrich) and stimulated with 2 μL of leukocyte activation cocktail (550583, BD Biosciences) in 5 % CO_2 at 37 °C for 4 h. Then, the cells were treated with anti-mouse CD3 (APC-Cy7-CD3, 1:200, 557596, BD Biosciences) and anti-mouse CD4 (BV510-CD4, 1:200, 563106, BD Biosciences) for 30 min and lysed in red blood cell lysis solution (130-094-183, Miltenyi Biotec) for 10 min. After being treated with fixation/permeabilization concentrate at room temperature for 1 h, total T lymphocytes were further stained with anti-mouse IFN-γ (FITC-IFN-γ, 1:100, 554411, BD Biosciences) and anti-mouse IL-4 (PE-IL-4, 1:100, 554435, BD Biosciences) for 30 min. Isotype controls were used for compensation and to confirm antibody specificity. Th1 cells were defined as $CD4^+IFN\text{-}\gamma^+$ cells, and Th2 cells were defined as $CD4^+IL\text{-}4^+$ cells. Data were acquired on a BD FACSCanto II and the flow cytometry data were analyzed using FlowJo

software.

2.7. Western blotting

Total protein was extracted from the mouse aortas (frozen at -80 °C) with RIPA lysis buffer (R0020, Solarbio). After incubation on ice for 10 min, all sample mixtures were centrifuged at 13,500 rpm for 15 min (4 °C) and their tissue supernatants were collected. Afterward, the protein concentration extracted from the mouse aortas was quantified with BCA protein concentration assay kit (P1511-1, Applygen). The protein sample extracts were mixed with SDS-PAGE protein loading buffer (1610747, Bio-rad). Then, their mixture is boiled for 5 min at 100 °C. The extracted protein was separated by SDS-PAGE, and transferred to nitrocellulose membranes at 250 mA for 1.5 h. The membranes were blocked with 5 % (w/v) nonfat dry milk in TBS containing 0.1 % (v/v) Tween 20 (TBS-T) for 1 h at room temperature (22–24 °C). The membranes were incubated with primary antibodies against phospho-IκBα (p-IκBα; 1:1000, 2859, Cell Signaling Technology), IκBα (1:1000, 4812, Cell Signaling Technology), phospho-p65 (p-p65; 1:1000, 3033, Cell Signaling Technology), p65 (1:1000, 8242, Cell Signaling Technology), and β-actin (1:1000, TA-09, Zsbio) overnight at 4 °C. After washing the membranes three times with TBS-T, they were incubated with goat anti-rabbit IRDye® 800 CW (1:10,000, P/N 926–32211, LI-COR Biosciences, Lincoln, USA) or goat anti-mouse IRDye® 680 RD (1:10,000, P/N 926–68070, LI-COR Biosciences) at room temperature for 1 h. The bands were quantified by using an Odyssey infrared imaging system (LI-COR Biosciences) and analyzed by Odyssey v3.0 software.

2.8. Real-time polymerase chain reaction (PCR)

Total RNA was extracted from aortas using TRIzol reagent (CW0580, CWBIO). NanoDrop-2000 Spectrophotometer (Thermo, USA) was used to measure total RNA concentration. Reverse transcription reactions were conducted according to the standard protocols provided by the High-Capacity cDNA Reverse Transcription Kit (4368813, Applied Biosystems). Reverse transcription was performed with a room temperature system protocol in a 20 μL reaction mixture as described previously [36,37]. Total RNA (1 μg) was used, and random primers were used to initiate cDNA synthesis. The reaction mixture was incubated at 25 °C for 10 min, 37 °C for 120 min and 85 °C for 5 min. Real-time PCR was performed on an ABI Prism 7500 sequence detection system using SYBR Green PCR core reagents (B21203, Bimake). PCR was performed according to the manufacturer's recommendations in a 20 μL reaction volume. Transcript levels were compared using the relative quantitation method, and the amount of detected mRNA was normalized to the amount of endogenous control (β-actin) mRNA. The expression level relative to that in the control sample was calculated by the $2^{-\Delta\Delta CT}$ method. The primer sequences are listed in Table 1.

2.9. RNA sequencing

Total aorta RNA was isolated, and RNA sequencing and data analysis were performed by Novogene Bioinformatics (Beijing, China). Total amounts and integrity of the aorta RNA were assessed through the Agilent Technologies Bioanalyzer 2100 system (CA, USA). The cDNA library construction, quality inspection, and clustering and sequencing were conducted based on the procedures by Novogene (Beijing, China). Differentially expressed genes (DEGs) were assessed with the following threshold: adjusted P value < 0.05 and $|\log 2$ Fold Change$| > 0.585$. Gene Ontology (GO) analysis was performed using the Protein with Values/Ranks Functional Enrichment Analysis online tool on the String 11.5 website, and GO items with FDR <0.05 were considered significantly enriched. The GO and Kyoto Encyclopedia of Genes and Genomes (KEGG) sets were independently used for Gene set enrichment analysis GSEA (GSEA). GSEA was performed via GSEA v4.1.0. The enrichment scores (ES) were calculated based on weighted Kolmogorov-Smirnov-like statistics. The data is available in the BioSample Submission Portal as BioProject PRJNA1147487 and Sequence Read Archive (SRA) accession number SRP525995.

2.10. Animal electrocardiogram (ECG)

The experimental conditions for ECG involved a quiet, clean laboratory at an appropriate temperature. The ECG machine was warmed up for 5 min and adjusted to eliminate baseline signal interference. Mice were anesthetized with isoflurane gas (0.8 % O_2, induction at 5 %, maintenance at 2 %, EZVET). During the procedure, mice were placed in the supine position, and electrodes were attached to all upper and lower limbs by gently piercing the needle under the skin. Baseline lead II ECGs were recorded before and after

Table 1
The primers used for real-time PCR to detect the target genes mRNAs.

Gene	Sense (5′–3′)	Antisense (5′–3′)
IFN-γ	GTACAACCTCCTTGCAGCTCCT	TTGTCGACGACGAGCGC
IL-4	CAGCTAGTTGTCATCCTGCTCTTC	GCCGATGATCTCTCTCAAGTGA
TNF-α	CGTCAGCCGATTTGCTATCT	CGGACTCCGCAAAGTCTAAG
IL-6	TTCCATCCAGTTGCCTTCTT	CAGAATTGCCATTGCACAAC
ICAM-1	TACTGCTGGTCATTGTGG	GGCTTGTCCCTTGAGTT
VCAM-1	TCTCCCAGGAATACAACGAT	ACAGGTCATTGTCACAGCAC
β-actin	ATCTGGCACCACACCTTC	AGCCAGGTCCAGACGCA

treatment using the BL-420F Biological Function Experiment System and analyzed by investigators blinded to the treatment [38].

2.11. Data analysis

Data were expressed as the mean ± SEM and were analyzed using GraphPad Prism Version 8.4 (GraphPad Software, San Diego, CA). For comparisons between two groups, significance was determined by Student's *t*-test. Multiple group comparisons were performed using one-way analysis of variance (ANOVA) followed by the Bonferroni corrected post hoc *t*-test. The results were considered significant at $P < 0.05$.

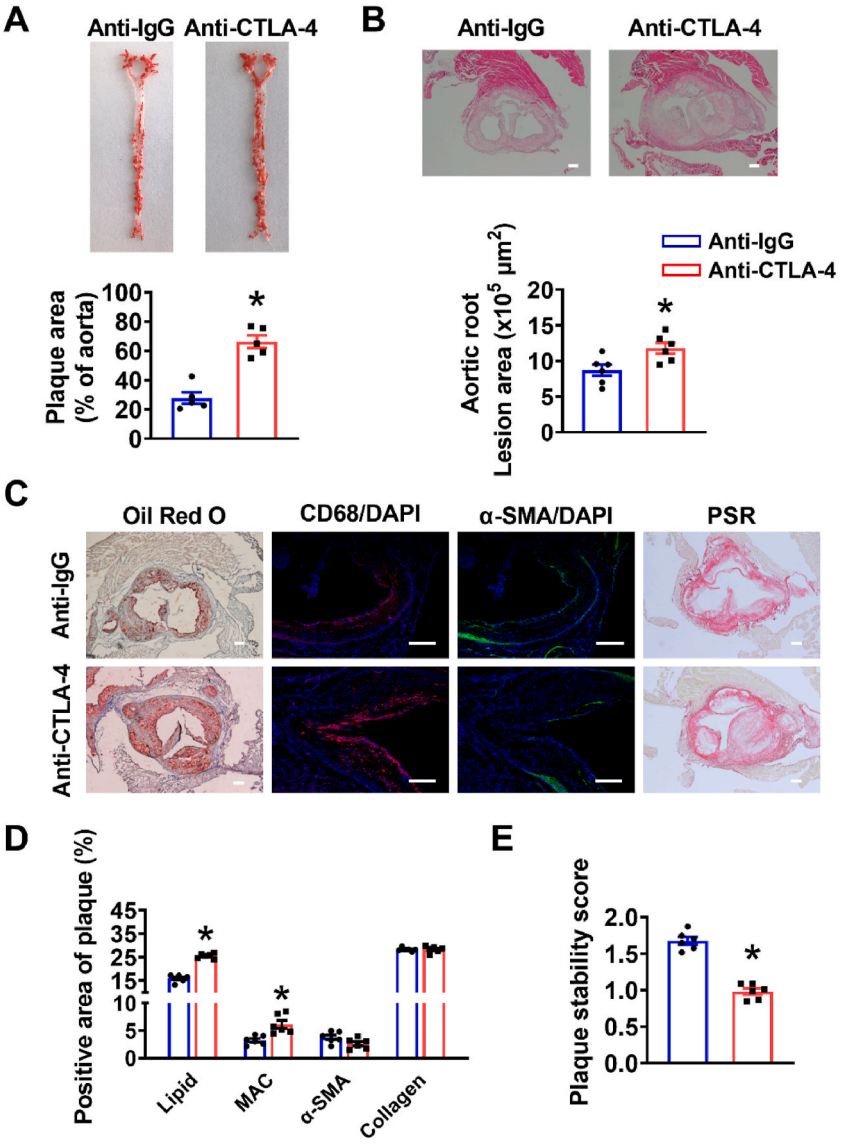

Fig. 1. The anti-CTLA-4 antibody exacerbates the atherosclerotic plaque area and reduces atherosclerotic plaque stability in the aortic root. (A) Representative images of ORO staining of en face aortic atherosclerotic lesions in the indicated groups (upper) and quantitative analysis of the atherosclerotic surface area of the entire aorta (lower). The data are presented as the means ± SEM (n = 5). **(B)** Representative H&E-stained images of aortic roots in the indicated groups (upper) and quantitative analysis of the lesion area in the aortic root (lower). Scale bar, 200 μm. The data are presented as the means ± SEM (n = 6). **(C)** Representative ORO, CD68, α-SMA and PSR staining images of aortic roots in the indicated groups. Scale bar, 200 μm. **(D)** Quantitative analysis of the percentage of the positive area in the aortic root. The data are presented as the means ± SEM (n = 6). **(E)** Quantitative analysis of the plaque stability score in the aortic root. The data are presented as the means ± SEM (n = 6). *P < 0.05 *vs.* the anti-IgG group.

3. Results

3.1. Anti-CTLA-4 antibody treatment exacerbates atherosclerotic plaque formation and decreases plaque stability in the aortic root of hyperlipidemic mice

To induce the atherosclerosis model, 6-week-old C57BL/6 mice were administered a single dose of AAV8-PCSK9 before being fed a PD. At 12 weeks, the mice were randomly injected with the IgG isotype or anti-CTLA-4 antibody twice per week for 4 consecutive weeks (Fig. S1A). There were no significant differences in body weight (Fig. S1B) or plasma lipid profiles, including TG, TC, LDL-C or HDL-C levels, between the two groups (Figs. S1C–1F). Atherosclerotic plaque formation was evaluated with en face ORO staining of the entire aorta. Compared with the anti-IgG group, the anti-CTLA-4 group exhibited a dramatic 2.38-fold increase in lipid accumulation (Fig. 1A). Furthermore, compared with the IgG group, the CTLA-4 group showed a significant increase in atherosclerotic lesion formation in the aortic root (Fig. 1B).

To further evaluate the progression and vulnerability of plaques, we investigated the composition of lesions in the aortic root, including the collagen content, smooth muscle cells, macrophage infiltration, and lipid accumulation, which contribute to plaque stability. The results showed that the anti-CTLA-4 antibody significantly increased macrophage infiltration and lipid accumulation, but the collagen-positive area and the number of smooth muscle cells did not significantly change (Fig. 1C and D). The plaque stability score, which assesses the collagen, macrophage, smooth muscle actin, and lipid composition of lesions, was lower in anti-CTLA-4-treated mice than in anti-IgG-injected mice (Fig. 1E). Taken together, these data demonstrate that antibody-mediated inhibition of CTLA-4 increases the atherosclerotic lesion area and promotes the progression of atherosclerotic plaques toward a more unstable plaque phenotype.

3.2. Anti-CTLA-4 antibody treatment exacerbates plaque progression and decreases plaque stability in the coronary artery

Next, we performed H&E staining on coronary arteries (Fig. 2A). Consistent with the findings in the aortic root, the results showed that anti-CTLA-4 antibody treatment increased the plaque area in the coronary arteries compared with those in the anti-IgG group (Fig. 2B). To further determine the effects of the anti-CTLA-4 antibody on plaque levels, we next performed immunohistochemical analysis of atherosclerotic lesions in the coronary artery. Notably, compared with those in the control group, the atherosclerotic lesions

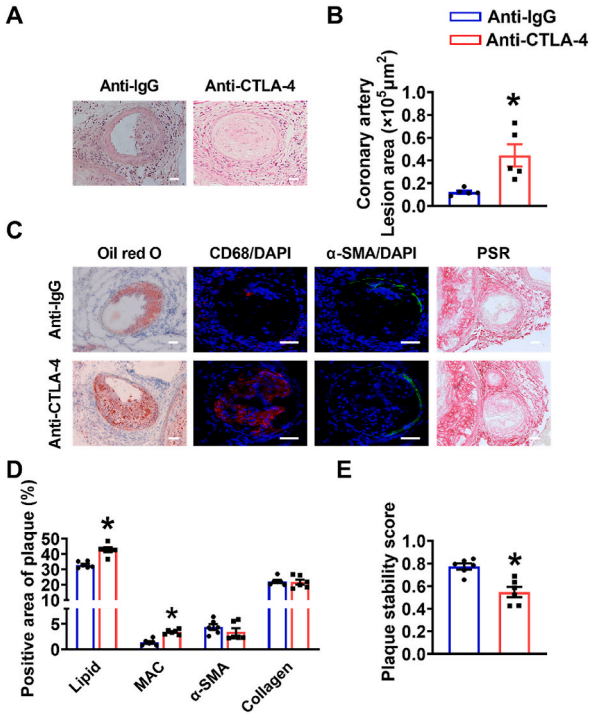

Fig. 2. The anti-CTLA-4 antibody exacerbates the atherosclerotic plaque area and reduces atherosclerotic plaque stability in the coronary artery. (A) Representative H&E-stained images of coronary arteries in the indicated groups. Scale bar, 50 μm. **(B)** Quantitative analysis of the lesion area in the coronary artery. The data are presented as the means ± SEM (n = 5). **(C)** Representative ORO, CD68, α-SMA and PSR staining images of coronary arteries in the indicated groups. Scale bar, 50 μm. **(D)** Quantitative analysis of the percentage of the positive area in the coronary artery. The data are presented as the means ± SEM (n = 6). **(E)** Quantitative analysis of the plaque stability score in the coronary artery. The data are presented as the means ± SEM (n = 6). *P < 0.05 *vs.* the anti-IgG group.

in the anti-CTLA-4 antibody group showed a marked increase in lipid accumulation, as assessed by ORO staining, and a significant increase in $CD68^+$ macrophage infiltration (Fig. 2C and D). The relative smooth muscle cell and collagen contents in the coronary artery plaques were not affected by the anti-CTLA-4 antibody (Fig. 2C and D). Compared with that in the anti-IgG group, the plaque stability score was decreased in the anti-CTLA-4 group (Fig. 2E). Therefore, we performed body surface electrocardiograms on the mice before and after injection. The results showed no significant variations in the anti-IgG group; however, 4 weeks after the injection of the anti-CTLA-4 antibody, the electrocardiograms showed ST-segment depression and altered T-wave inversion in the mice in the anti-CTLA-4 group (incidence of 3/11, Fig. S2). These data suggest that anti-CTLA-4 antibody treatment causes myocardial ischemic lesions in hyperlipidemic mice. Taken together, these data demonstrate that anti-CTLA-4 therapy exacerbates plaque progression in both the aortic root and coronary artery.

3.3. Anti-CTLA-4 antibody treatment promotes $CD4^+$ T-cell infiltration in the aortic root in hyperlipidemic mice

To gain further insight into the expression of genes that were altered in hyperlipidemic mice in response to anti-CTLA-4 antibody treatment, we analyzed the aortas by RNA sequencing. The GO results showed that the DEGs were markedly enriched in the biological process of positive regulation of T-cell activation (Fig. 3A). To evaluate the effect of the anti-CTLA-4 antibody on plaque $CD4^+$ T-cell infiltration, we used immunofluorescence staining to analyze the infiltration of $CD4^+$ T cells in the plaque area of the aortic root. The results showed that the anti-CTLA-4 antibody promoted $CD4^+$ T-cell infiltration in the aortic root (Fig. 3C and D). Taken together, these data demonstrate that the increased accumulation of T cells within lesions is associated with accelerated plaque growth caused by anti-CTLA-4 antibody treatment.

3.4. Anti-CTLA-4 antibody treatment promotes Th1 polarization during atherosclerosis

To further understand the reasons underlying the anti-CTLA-4 antibody-induced increase in T-cell infiltration in the aortic root, we performed GSEA of the microarray data. The results showed that "regulation of Th1-type immune response" and "Th1 cell differentiation" were enriched in the anti-CTLA-4 group (Fig. 3B). The Th1/Th2 balance controls inflammation and plays an important role in atherosclerosis [20].The pools of Th1 and Th2 cells were estimated by quantifying the proportions of peripheral blood $CD4^+$ T cells that could produce IFN-γ and IL-4, respectively, in response to stimulation. In anti-CTLA-4-treated mice, the pool of Th1 cells was increased, and the pool of Th2 cells was unaffected by anti-CTLA-4 antibody treatment, as determined by flow cytometry (Fig. 3E and F). The Th1/Th2 ratio, which was estimated by determining the $CD4^+IFN\text{-}\gamma^+IL\text{-}4^-$ cell/$CD4^+IFN\text{-}\gamma^-IL\text{-}4^+$ cell ratio, was significantly higher in the anti-CTLA-4 group than in the anti-IgG group (Fig. 3G), demonstrating a shift in the Th balance toward Th1-dominant immune responses. In addition, IFN-γ and IL-4 levels in the aorta were measured by real-time PCR. Higher IFN-γ levels and lower IL-4 levels were observed in the anti-CTLA-4 group than in the anti-IgG group (Fig. 3H). Additionally, co-immunofluorescent staining demonstrated a significant increase in the number of $CD4^+IFN\text{-}\gamma^+$ T cells in the plaque area of the aortic root following anti-CTLA-4 antibody treatment, whereas the number of $CD4^+IL\text{-}4^+$ T cells decreased with CTLA-4 intervention (Fig. 3I and J and Fig. S3). Taken together, these data demonstrate that the anti-CTLA-4 antibody promotes T-cell infiltration and causes a Th1/Th2 imbalance.

3.5. Anti-CTLA-4 antibody treatment activates the NF-κB signaling pathway

GSEA revealed that the anti-CTLA-4 antibody activated NF-κB, which is a nuclear transcription factor that regulates proinflammatory cytokine expression (Fig. 4A). IκBα is attached to the p50-p65 heterodimer complex, and when IκBα is phosphorylated and subsequently degraded, phosphorylated p65 translocates to the nucleus and becomes activated [39,40]. Western blotting revealed that the anti-CTLA-4 antibody increased the levels of phosphorylated IκBα and p65 (Fig. 4B–E). In addition, we investigated whether the anti-CTLA-4 antibody was involved in inflammatory responses and endothelial adhesion molecule production in mouse aortas. As shown in Fig. 4F, the anti-CTLA-4 antibody significantly increased the mRNA levels of proinflammatory cytokines, including TNF-α and IL-6, and endothelial adhesion molecules, including ICAM-1 and VCAM-1 (Fig. 4F). These results suggest that the anti-CTLA-4 antibody could activate the NF-κB signaling pathway, contributing to the increase in proinflammatory cytokines and the production of endothelial adhesion molecules.

3.6. NF-κB inhibition attenuates the exacerbation of atherosclerotic plaques induced by anti-CTLA-4 antibody treatment

Subsequently, we performed in vivo experiments to determine whether the NF-κB signaling pathway played a key role in the acceleration of atherosclerosis induced by the anti-CTLA-4 antibody. BAY11-7082 is an inhibitor of IκBα phosphorylation and the subsequent activation of NF-κB [41]. MG132 (Z-Leu-Leu-Leu-aldehyde) is a peptide aldehyde proteasome inhibitor that inhibits the degradation of IκBα, resulting in the suppression of NF-κB activation [42]. Therefore, the mice were intraperitoneally injected with the anti-CTLA-4 antibody plus MG132 or BAY11-7082 to examine whether inhibiting NF-κB activation could attenuate the atherosclerotic effect of anti-CTLA-4 antibody. The protein expression of phosphorylated IκBα and p65 in the aorta was examined by western blotting. The results showed that the anti-CTLA-4 antibody activated NF-κB signaling, as indicated by increased phosphorylation of IκBα and p65, and this effect was reversed by MG132 or BAY11-7082 coinjection (Fig. 5A–C and Fig. 6A–C), indicating that MG132 or BAY11-7082 could inhibit the NF-κB signaling pathway. Subsequently, atherosclerotic plaques in the aorta were examined by ORO staining. Compared with those in the anti-CTLA-4 group, the areas of atherosclerotic plaques in the aorta were reduced in the anti-CTLA-4 + MG132 group (Fig. 5D) and the anti-CTLA-4 + BAY11-7082 group (Fig. 6D). Furthermore, the plaque area in the aortic

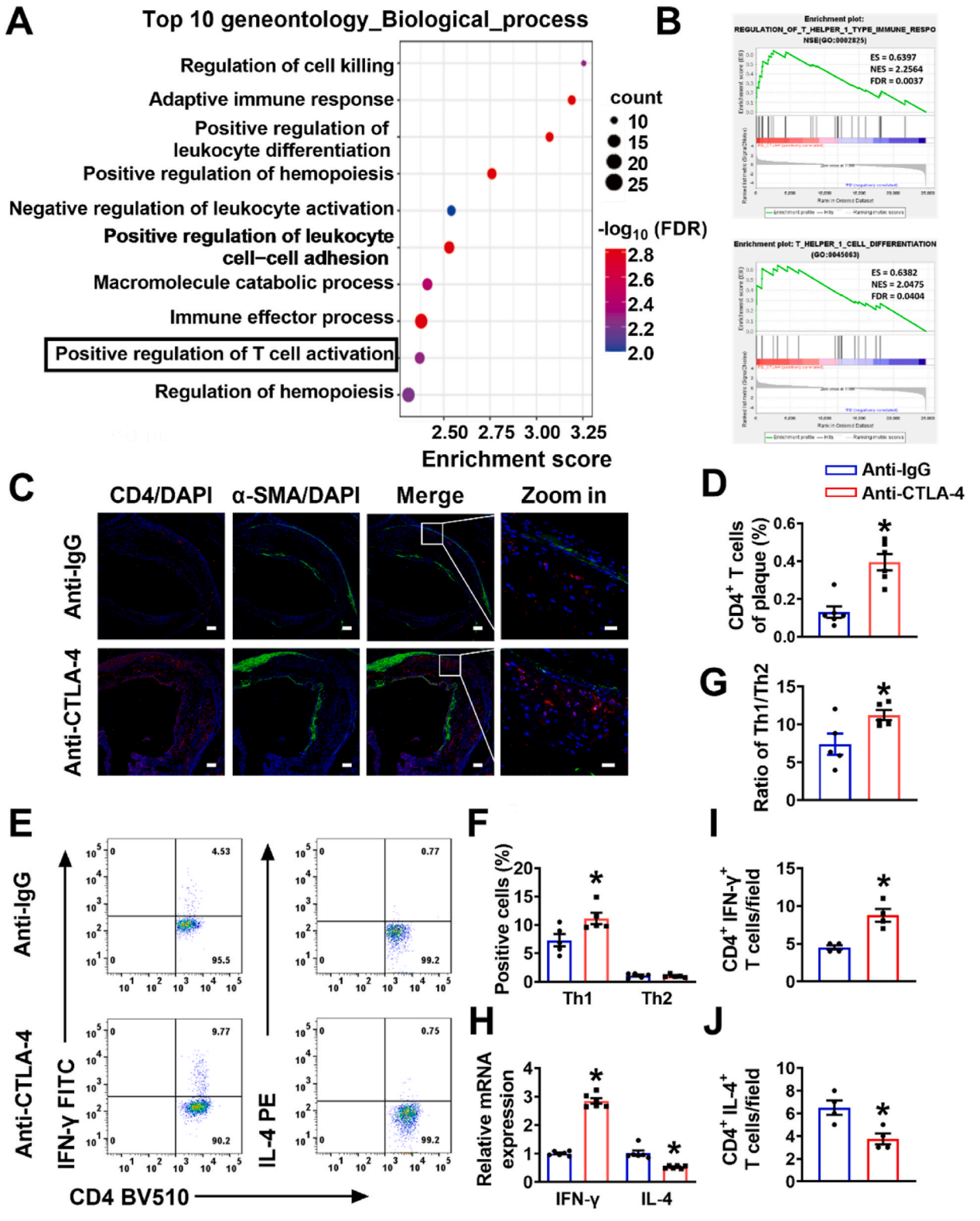

(caption on next page)

Fig. 3. The anti-CTLA-4 antibody promotes $CD4^+$ T-cell infiltration and T-cell differentiation into Th1 cells in the aortic root. (A) GO enrichment analysis showing the significantly enriched biological processes in hyperlipidemic mice administered the anti-IgG antibody or anti-CTLA-4 antibody. n = 3 per group. **(B)** GSEA of RNA-seq data showing the enrichment of "regulation of Th1-type immune response" and "Th1 cell differentiation" in hyperlipidemic mice administered the anti-IgG antibody or anti-CTLA-4 antibody. NES: normalized enrichment score; FDR: adjusted p value. **(C)** Representative immunofluorescence staining of CD4 (red), α-SMA (green), and DAPI (blue) in mice in the indicated groups. The square represents the colocalization of CD4 with the smooth muscle marker α-SMA. The scale bars are 100 μm and 20 μm. **(D)** Quantitative analysis of CD4 fluorescence intensity in aortic roots in the indicated groups. The data are presented as the means ± SEM (n = 6). **(E)** Flow cytometric analysis of the distributions of $CD4^+IFN\text{-}\gamma^+$ T cells and $CD4^+IL\text{-}4^+$ T cells in peripheral blood in the indicated groups. **(F)** Relative quantification of the percentages of $CD4^+IFN\text{-}\gamma^+$ T cells and $CD4^+IL\text{-}4^+$ T cells among the sorted $CD4^+$ T cells. The data are presented as the means ± SEM (n = 5). **(G)** The Th1/Th2 ratio was estimated by determining the ratio of $CD4^+IFN\text{-}\gamma^+IL\text{-}4^-$ cells to $CD4^+IFN\text{-}\gamma^-IL\text{-}4^+$ cells. The data are presented as the means ± SEM (n = 5). **(H)** Quantitative results were obtained by real-time PCR showing the relative mRNA expression of IFN-γ and IL-4 in the indicated groups. The data are presented as the means ± SEM (n = 6). *P < 0.05 *vs.* the anti-IgG group. **(I–J)** Quantitative analyses demonstrating the number of $CD4^+IFN\text{-}\gamma^+$ T cells and $CD4^+IL\text{-}4^+$ T cells in aortic roots from each indicated experimental group. The data are presented as the means ± SEM (n = 4). *P < 0.05 *vs.* the anti-IgG group.

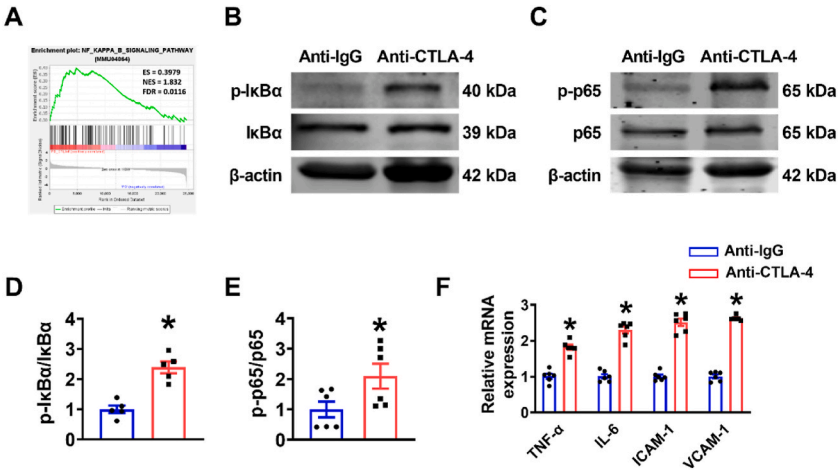

Fig. 4. The anti-CTLA-4 antibody activates the NF-κB signaling pathway. (A) GSEA of RNA-seq data showing enrichment of the "NF-κB signaling pathway" in hyperlipidemic mice administered the anti-IgG antibody or anti-CTLA-4 antibody. **(B)** Representative western blots and **(D)** quantification of p-IκBα and IκBα. β-actin was used as an internal control. The data are presented as the means ± SEM (n = 5). **(C)** Representative western blots and **(E)** quantification of p-p65 and p65. The data are presented as the means ± SEM (n = 6). **(F)** Quantification of the results obtained by real-time PCR showing the relative mRNA expression of TNF-α, IL-6, ICAM-1 and VCAM-1 in the indicated groups. The data are presented as the means ± SEM (n = 6). *P < 0.05 *vs.* the anti-IgG group.

root was also reduced in the anti-CTLA-4 + MG132 group (Fig. 5E) and the anti-CTLA-4 + BAY11-7082 group (Fig. 6E). Overall, NF-κB inhibitors attenuate the aggravation of atherosclerotic plaque formation induced by the anti-CTLA-4 antibody.

3.7. NF-κB inhibition ameliorates T-cell differentiation to Th1 cells induced by anti-CTLA-4 antibody treatment

To determine the relationship between the NF-κB signaling pathway and T-cell differentiation in anti-CTLA-4 antibody-mediated atherosclerosis, the percentages of Th1 cells and Th2 cells in peripheral blood were examined by flow cytometry. The results showed that the Th1/Th2 ratio was increased in the anti-CTLA-4 group, and this effect was alleviated by MG132 or BAY11-7082 treatment (Fig. 5F–H and 6F-6H). In addition, we analyzed the mRNA expression levels of IFN-γ and IL-4 in the aorta by real-time PCR. Compared with that in the anti-CTLA-4 group, the expression of IFN-γ in the aorta was reduced, and the expression of IL-4 was increased in the anti-CTLA-4 + MG132 groups and anti-CTLA-4 + BAY11-7082 (Figs. 5I and 6I). Overall, MG132 or BAY11-7082 attenuated the anti-CTLA-4 antibody-induced acceleration of atherosclerotic plaque progression and ameliorated T-cell differentiation to Th1 cells, suggesting that the NF-κB signaling pathway plays an important role in the anti-CTLA-4 antibody-mediated aggravation of atherosclerosis in hyperlipidemic mice.

4. Discussion and limitations

Here, we reported that (1) anti-CTLA-4 antibody treatment exacerbated experimental atherosclerosis by accelerating the progression of initial plaques toward more advanced and unstable lesions in both the aortic roots and coronary arteries; (2) blockade of CTLA-4 enhanced $CD4^+$ T-cell infiltration and increased the Th1/Th2 ratio, indicating strong T-cell-driven inflammation; and (3) inhibiting NF-κB ameliorated the anti-CTLA-4 antibody-mediated exacerbation of plaque progression and Th1/Th2 imbalance.

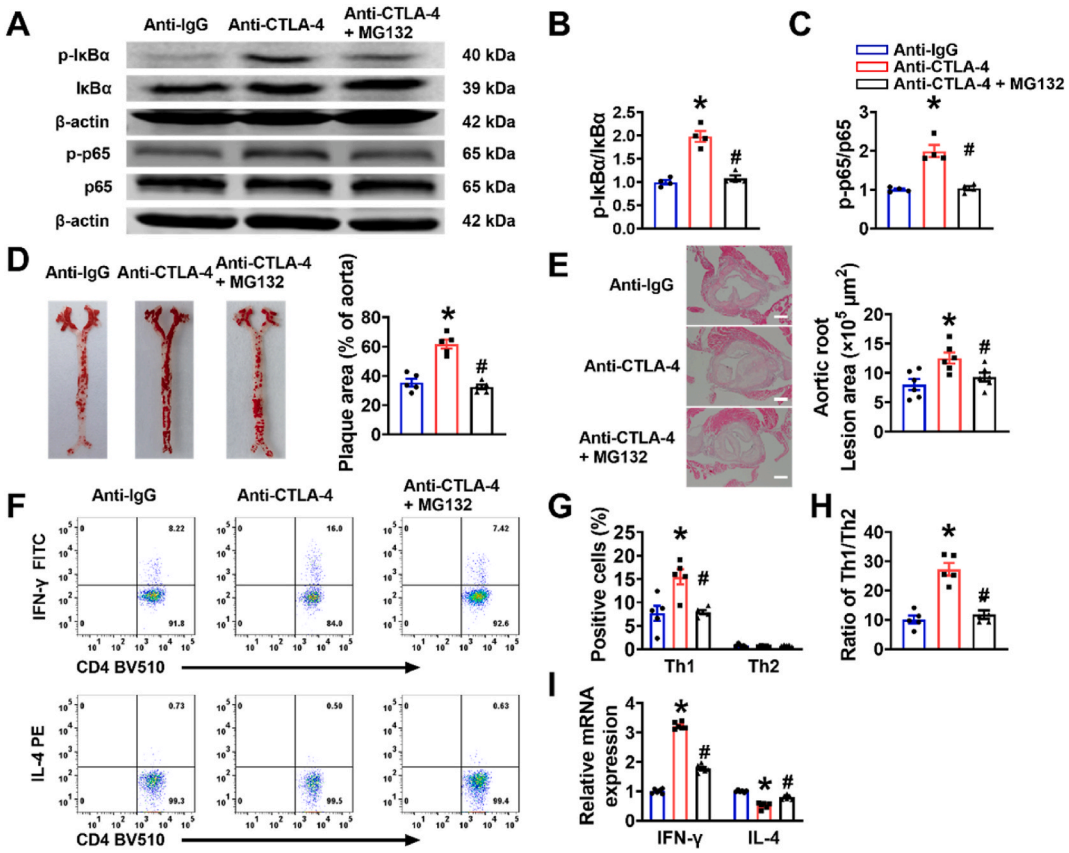

Fig. 5. MG132 attenuates the aggravation of atherosclerotic plaques induced by the anti-CTLA-4 antibody. (A) Representative western blots of p-IκBα, IκBα, p-p65, and p65. **(B)** Quantification of p-IκBα and IκBα. β-actin was used as an internal control. The data are presented as the means ± SEM (n = 4). **(C)** Quantification of p-p65, and p65. β-actin was used as an internal control. The data are presented as the means ± SEM (n = 4). **(D)** Representative images of ORO staining of en face aortic atherosclerotic lesions in the indicated groups (left) and quantitative analysis of the atherosclerotic surface area of the entire aorta (right). The data are presented as the means ± SEM (n = 5). **(E)** Representative H&E-stained images of aortic roots in the indicated groups (left) and quantitative analysis of the lesion area in aortic roots (right). Scale bar, 200 μm. The data are presented as the means ± SEM (n = 6). **(F)** Flow cytometric analysis of $CD4^+IFN\text{-}\gamma^+$ T-cell and $CD4^+IL\text{-}4^+$ T-cell distributions in peripheral blood in the indicated groups. **(G)** Relative quantification of the percentages of $CD4^+IFN\text{-}\gamma^+$ T cells and $CD4^+IL\text{-}4^+$ T cells among the sorted $CD4^+$ T cells. The data are presented as the means ± SEM (n = 5). **(H)** The Th1/Th2 ratio was estimated based on the ratio of $CD4^+IFN\text{-}\gamma^+IL\text{-}4^-$ cells to $CD4^+IFN\text{-}\gamma^-IL\text{-}4^+$ cells. The data are presented as the means ± SEM (n = 5). **(I)** Quantification of the results obtained by real-time PCR showing the relative mRNA expression of IFN-γ and IL-4 in the indicated groups. The data are presented as the means ± SEM (n = 6). *P < 0.05 *vs*. the anti-IgG group; #P < 0.05 *vs*. the anti-CTLA-4 group.

Recent clinical evidence has suggested an increase in atherosclerotic cardiovascular disease (ASCVD) in patients receiving ICI therapy. In a single-center, matched cohort study, patients receiving ICIs had a threefold increased risk of cardiovascular events involving accelerated progression of atherosclerosis [12]. However, to date, no drugs are clinically available to target ASCVD triggered by ICI therapy, and the specific mechanisms by which anti-CTLA-4 antibodies accelerate atherosclerosis remain unclear. Therefore, we used a single intravenous administration of AAV8-PCSK9, which is a convenient and efficient method that leads to rapid and enduring hyperlipidemia and atherosclerosis, to establish an atherosclerosis model. Compared with other transgenic mice, this approach allows for the tissue-specific expression of disease-causing mutated genes in wild-type (WT) mice, eliminating the necessity for intricate backcrosses, nonnatural gene mutations, and the upkeep of extensive populations of genetically modified animals [43,44]. Several immune cell types contribute to the development of atherosclerosis, with macrophages and T cells being the most prominent. Additionally, the inflammatory factors associated with these immune cells are linked to myocardial fibrosis, heart failure, and other related diseases [45]. Studies have shown that Tanshinone IIA may treat atherosclerosis by enhancing macrophage efferocytosis to reduce lipid accumulation [46]. We investigated the composition and stability of plaques in the aortic and coronary plaque areas after treatment with anti-IgG and anti-CTLA-4 antibodies. We found that the anti-CTLA-4 antibody increased atherosclerotic lesion size and promoted $CD4^+$ T-cell and $CD68^+$ macrophage infiltration at the aortic root, suggesting that anti-CTLA-4 antibody may enlarge the size of atherosclerotic plaques by promoting the infiltration of immune cells.

Coronary artery disease , caused by atherosclerosis, is a prominent cause of morbidity and mortality globally. The pathogenesis involves dysregulation of lipid metabolism and an aberrant immune response, leading to chronic inflammation of the arterial wall [47,

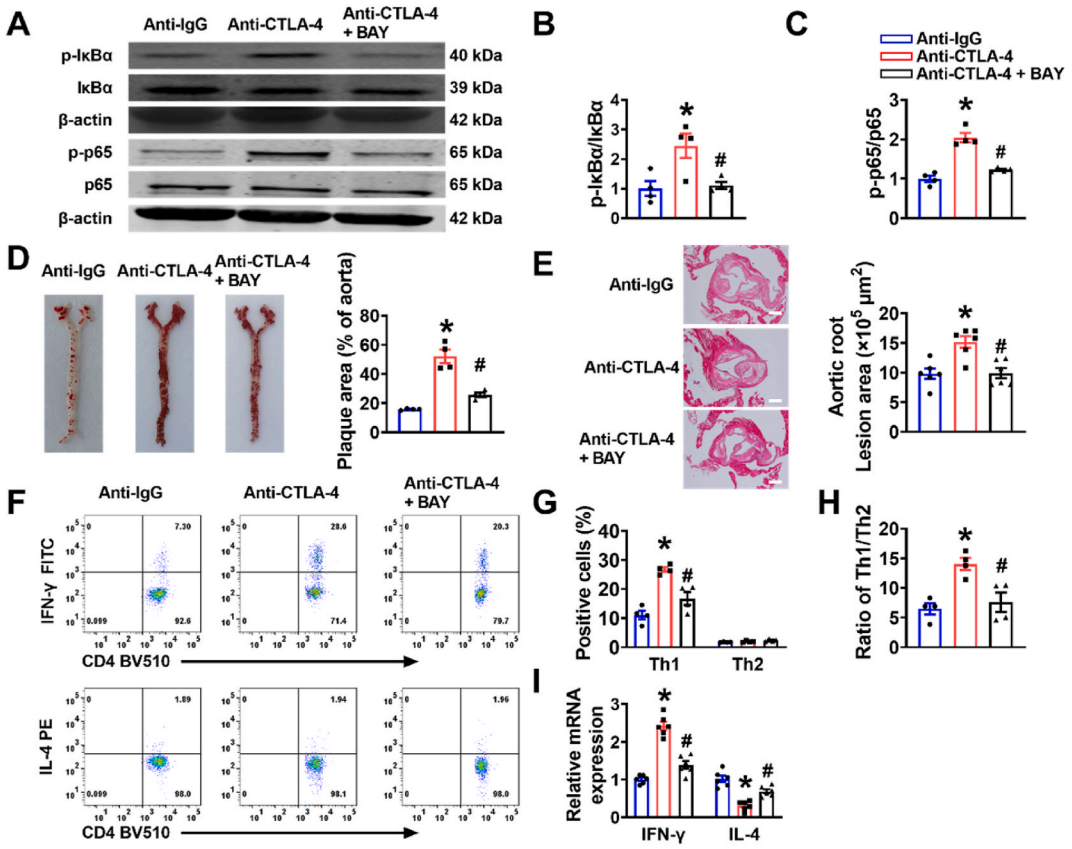

Fig. 6. BAY11-7082 ameliorates the aggravation of atherosclerotic plaques caused by the anti-CTLA-4 antibody. (A) Representative western blots of p-IκBα, IκBα, p-p65, and p65. (B) Quantification of p-IκBα and IκBα. β-actin was used as an internal control. The data are presented as the means ± SEM (n = 4). (C) Quantification of p-p65, and p65. β-actin was used as an internal control. The data are presented as the means ± SEM (n = 4). **(D)** Representative images of ORO staining of en face aortic atherosclerotic lesions in the indicated groups (left) and quantitative analysis of the atherosclerotic surface area of the entire aorta (right). The data are presented as the means ± SEM (n = 4). **(E)** Representative H&E-stained images of aortic roots in the indicated groups (left) and quantitative analysis of the lesion areas in aortic roots (right). Scale bar, 200 μm. The data are presented as the means ± SEM (n = 6). **(F)** Flow cytometric analysis of $CD4^+IFN\text{-}\gamma^+$ T-cell and $CD4^+IL\text{-}4^+$ T-cell distributions in peripheral blood in the indicated groups. **(G)** Relative quantification of the percentages of $CD4^+IFN\text{-}\gamma^+$ T cells and $CD4^+IL\text{-}4^+$ T cells among the sorted $CD4^+$ T cells. The data are presented as the means ± SEM (n = 4). (**H**) The Th1/Th2 ratio was estimated by determining the ratio of $CD4^+IFN\text{-}\gamma^+IL\text{-}4^-$ cells to $CD4^+IFN\text{-}\gamma^-IL\text{-}4^+$ cells. The data are presented as the means ± SEM (n = 4). **(I)** Quantification of the results obtained by real-time PCR showing the relative mRNA expression of IFN-γ and IL-4 in the indicated groups. The data are presented as the means ± SEM (n = 6). *P < 0.05 *vs.* the anti-IgG group; #P < 0.05 *vs.* the anti-CTLA-4 group.

48]. T-cell-mediated inflammation plays a pivotal role in the initiation and progression of atherosclerosis [16]. CTLA-4, a crucial negative regulator of T cell activation, has been implicated in modulating the infiltration of T cells and inflammatory mediators, albeit without affecting lipid profiles. Matsumoto et al. [14] reported that CTLA-4 overexpression in $Apoe^{-/-}$ mice could reduce atherosclerosis by decreasing plaque inflammation, as evidenced by a 38 % decrease in macrophage accumulation, a 42 % decrease in $CD4^+$ T-cell infiltration and a decrease in T-cell proliferation and proinflammatory cytokine production. In addition, the results showed that there were no significant differences in the plasma lipid profile between male or female control $Apoe^{-/-}$ and CTLA-4-Tg/$Apoe^{-/-}$ mice [14]. Similarly, mice with increased homocysteine levels had larger atherosclerotic plaque sizes associated with decreased CTLA-4 expression, and pretreatment of these mice with CTLA-4-IgG (abatacept) ameliorated plaque development, reduced IFN-γ and IL-2 production and decreased macrophage levels, without influence plasma cholesterol or triglyceride levels in $Apoe^{-/-}$ mice [49]. Our findings consistently demonstrated that CTLA-4 inhibition does not affect lipid profiles; however, it does promote $CD4^+$ T-cell infiltration in the aortic root and enhances atherosclerotic plaque formation in mice injected with AAV8-PCSK9 and fed with a Paigen diet.

We also reported that a Th1 bias in the Th1/Th2 immune response may play an important role, as determined by measuring the levels of Th1 and Th2 cytokines such as IFN-γ and IL-4. Th1 cells produce IFN-γ, which promotes the formation of foam cells and accelerates the development of plaques, whereas Th2 cells produce anti-inflammatory factors, such as IL-4, IL-5, and IL-13 [50]. Suppressing Th1 function or enhancing Th2 function has been shown to reduce atherogenesis in $Apoe^{-/-}$ or LDL receptor-deficient mice [16]. In an in-situ mouse model of highly aggressive colon cancer, the mRNA and protein levels of IL-1α and IFN-γ were

significantly upregulated following treatment with anti-CTLA-4 antibody. Conversely, the expression of IL-4 protein exhibited a slight decrease [51]. CTLA-4 haploinsufficiency is a Mendelian syndrome characterized by T cell overactivation and autoimmunity, often leading to paradoxical and unexplained hypogammaglobulinemia and a decline in B cells [52,53]. The study demonstrated that in the peripheral blood of patients with CTLA-4 haploinsufficiency, the proportion of cells producing IFN-γ increased, while the proportion of IL-17A-producing cells decreased. In contrast, the proportions of cells producing IL-4 and IL-21 were not different from those of healthy donors [54]. These findings suggest that CTLA-4 inhibition is associated with Th1 cell differentiation. Therefore, we hypothesized that the development of atheromatous plaques in anti-CTLA-4 antibody-treated mice involved modulating the Th1/Th2 balance. In the present study, RNA sequencing and GO analyses revealed that the DEGs were notably enriched in the biological process of positive regulation of T-cell activation. In addition, the GSEA showed that "regulation of Th1-type immune response" and "Th1 cell differentiation" were enriched in the anti-CTLA-4 group. Substantial evidence suggests that the Th1/Th2 balance controls inflammation and may therefore be important in the development of atherosclerosis [55]. Here, we assessed whether anti-CTLA-4 antibody treatment modulated the Th1/Th2 balance in hyperlipidemic mice by examining $CD4^{+}IFN\text{-}\gamma^{+}$ T cells and $CD4^{+}IL\text{-}4^{+}$ T cells in both peripheral blood and aortic plaque. Our results showed that Th1/Th2 ratios were higher in the anti-CTLA-4 antibody-treated group than in the anti-IgG group, which suggested that the anti-CTLA-4 antibody promoted T-cell differentiation toward the Th1 type.

IFN-γ stimulates the production of cytokines, which are crucial protein mediators of inflammation, and increases the expression of adhesion molecules on vascular endothelial cells [55]. Our data showed that the mRNA expression levels of TNF-α, IL-6, ICAM-1 and VCAM-1 in aortas were significantly increased by anti-CTLA-4 antibody injection in mice. Furthermore, Th1 cell-derived IFN-γ may have other effects that are directly linked to atherosclerosis. In particular, Th1 cells secrete IFN-γ to induce M1 macrophage polarization, and Th2 cells secrete IL-4 to induce M2 macrophage polarization. The hallmark pathology of atherosclerosis is the accumulation of activated M1 macrophages in coronary arteries, which initiate and sustain inflammation and are incapable of digesting lipids, thereby resulting in foam cell formation in atherosclerotic plaques [56]. Therefore, our results suggest that therapy with anti-CTLA-4 antibodies has the potential to modulate the Th1/Th2 balance and facilitate the development of atherosclerotic plaques, without affecting lipid levels.

NF-κB proteins are a family of ubiquitous transcription factors that regulate the response to cellular stress and mediate innate and adaptive immunity through the initiation of inflammatory responses induced by proinflammatory signals [57,58]. Atherosclerosis is an inflammatory condition in which NF-κB signaling has been implicated [59–61]. Based on the RNA-seq results, we determined the effects of the anti-CTLA-4 antibody on the NF-κB pathway. Our results showed that compared with those in the anti-IgG group, the protein expression levels of p-IκBα and p-p65 were significantly increased in the anti-CTLA-4 antibody-treated group. NF-κB activation is thought to cause concomitant alterations in the Th1 and Th2 transcription factors T-bet and GATA-3 and their respective cytokines, IFN-γ and IL-4 [62]. The present data indicated that MG132 or BAY11-7082 attenuated the anti-CTLA-4 antibody-induced acceleration of atherosclerotic plaque progression and ameliorated T-cell differentiation into Th1 cells, suggesting that modulating the Th1/Th2 balance via NF-κB signaling has a beneficial effect on the inflammatory process in lesion sites.

Our study has several limitations: 1) We utilized a tumor-free atherosclerosis model in mice, which may not fully represent the development of anti-CTLA-4- exacerbated atherosclerosis in patients. Using a tumor-bearing atherosclerosis model could enhance the translational relevance of our findings, given the common pathophysiological pathways shared between atherosclerosis and cancer, such as inflammation. 2) In our flow cytometry experiment, we only examined the Th1/Th2 ratio in the peripheral blood of mice; further research is needed to investigate the specific numbers of T cell subtypes in the aorta. 3) The therapeutic potential of MG132 and BAY11-7082 in cancer therapy has been assessed [63,64], and the next experiment should further investigate whether the combination of MG132 or BAY11-7082 with anti-CTLA-4 antibody exhibits a synergistic therapeutic effect in tumor-bearing mice. Future studies are expected to offer deeper insights into the pathological mechanisms of ASCVD exacerbated by anti-CTLA-4 therapy, and to establish a theoretical foundation for the clinical use of NF-κB pathway inhibitors such as MG132 and BAY11-7082.

5. Conclusion

In summary, anti-CTLA-4 antibody treatment increased aortic and coronary plaque progression and decreased plaque stability in hyperlipidemic mice by activating the NF-κB signaling pathway and subsequently promoting T-cell differentiation into Th1 cells. MG132 and BAY11-7082 attenuated the anti-CTLA-4 antibody-induced acceleration of atherosclerotic plaque progression by inhibiting the NF-κB signaling pathway and T-cell differentiation into Th1 cells. Our results provide a new therapeutic target and potential strategy for the treatment of adverse cardiovascular events during ICI administration.

Ethics statement

The use of animals and the experimental procedures were approved by the Ethics Committees of the First Affiliated Hospital of Harbin Medical University (2020122) and conformed to the Guide for the Care and Use of Laboratory Animals published by the US National Institutes of Health.

Data availability statement

Data will be made available from corresponding author upon reasonable request.

Sources of funding

This work was generously supported by grants from the National Natural Science Foundation of China (Nos. 81930009, 82230008, and 81870370 to Zhi-Ren Zhang; 81800513 to Chang-Jiang Yu), the Nn10 Program of Harbin Medical University Cancer Hospital (to Zhi-Ren Zhang), Natural Science Fund Research Team Project of Heilongjiang Provincial Department of Science and Technology (TD2023H001 to Zhi-Ren Zhang), and the Outstanding Youth Fund of Harbin Medical University Cancer Hospital (No. JCQN2020-02 to Chang-Jiang Yu).

CRediT authorship contribution statement

Ming-Luan Zhao: Writing – review & editing, Writing – original draft, Visualization, Project administration, Methodology, Investigation, Formal analysis, Data curation. **Chen Liang:** Writing – review & editing, Writing – original draft, Visualization, Validation, Supervision, Formal analysis, Data curation. **Wei-Wei Jiang:** Visualization, Project administration, Investigation, Formal analysis, Data curation. **Mei Zhang:** Project administration, Investigation. **Hong Guan:** Project administration, Investigation. **Zi Hong:** Project administration, Investigation. **Di Zhu:** Project administration, Investigation. **An-Qi Shang:** Project administration, Investigation. **Chang-Jiang Yu:** Writing – review & editing, Funding acquisition, Data curation. **Zhi-Ren Zhang:** Writing – review & editing, Supervision, Resources, Funding acquisition, Conceptualization.

Declaration of competing interest

The authors declare that they have no known competing financial interests or personal relationships that could have appeared to influence the work reported in this paper.

Acknowledgment

We would like to express our gratitude to Crystal Song Zhang for her contributions to this article, which include proofreading, language revision, and supplementary experiments.

Appendix A. Supplementary data

Supplementary data to this article can be found online at https://doi.org/10.1016/j.heliyon.2024.e37278.

References

[1] L. Zhang, X. Huang, Y. Gao, X. Li, Q. Kong, Y. Chen, J. Chang, G. Zhang, Y. Ma, Herbal formulas for detoxification and dredging collaterals in treating carotid atherosclerosis: a systematic review and meta-analysis, Front. Pharmacol. 14 (2023) 1147964.
[2] J. Chen, Z. Tang, Z. Chen, Y. Wei, H. Liang, X. Zhang, Z. Gao, H. Zhu, MicroRNA-218-5p regulates inflammation response via targeting TLR4 in atherosclerosis, BMC Cardiovasc. Disord. 23 (2023) 122.
[3] Q. Meng, H. Liu, J. Liu, Y. Pang, Q. Liu, Advances in immunotherapy modalities for atherosclerosis, Front. Pharmacol. 13 (2022) 1079185.
[4] J. Jing, J. Guo, R. Dai, C. Zhu, Z. Zhang, Targeting gut microbiota and immune crosstalk: potential mechanisms of natural products in the treatment of atherosclerosis, Front. Pharmacol. 14 (2023) 1252907.
[5] W. In Het Panhuis, M. Schonke, M. Modder, H.E. Tom, R.A. Lalai, A.C.M. Pronk, T.C.M. Streefland, L.W.M. van Kerkhof, M.E.T. Dolle, M.A.C. Depuydt, I. Bot, W. G. Vos, L.A. Bosmans, B.W. van Os, E. Lutgens, P.C.N. Rensen, S. Kooijman, Time-restricted feeding attenuates hypercholesterolaemia and atherosclerosis development during circadian disturbance in APOE *3-Leiden.CETP mice, EBioMedicine 93 (2023) 104680.
[6] W. Tong, Y. Zhang, H. Hui, X. Feng, B. Ning, T. Yu, W. Wang, Y. Shang, G. Zhang, S. Zhang, F. Tian, W. He, Y. Chen, J. Tian, Sensitive magnetic particle imaging of haemoglobin degradation for the detection and monitoring of intraplaque haemorrhage in atherosclerosis, EBioMedicine 90 (2023) 104509.
[7] E. Nunez, V. Fuster, M. Gomez-Serrano, J.M. Valdivielso, J.M. Fernandez-Alvira, D. Martinez-Lopez, J.M. Rodriguez, E. Bonzon-Kulichenko, E. Calvo, A. Alfayate, M. Bermudez-Lopez, J.C. Escola-Gil, L. Fernandez-Friera, I. Cerro-Pardo, J.M. Mendiguren, F. Sanchez-Cabo, J. Sanz, J.M. Ordovas, L.M. Blanco-Colio, J.M. Garcia-Ruiz, B. Ibanez, E. Lara-Pezzi, A. Fernandez-Ortiz, J.L. Martin-Ventura, J. Vazquez, Unbiased plasma proteomics discovery of biomarkers for improved detection of subclinical atherosclerosis, EBioMedicine 76 (2022) 103874.
[8] N.I. Dmitrieva, A. Gagarin, D. Liu, C.O. Wu, M. Boehm, Middle-age high normal serum sodium as a risk factor for accelerated biological aging, chronic diseases, and premature mortality, EBioMedicine 87 (2023) 104404.
[9] C. Li, R. Liu, Z. Xiong, X. Bao, S. Liang, H. Zeng, W. Jin, Q. Gong, L. Liu, J. Guo, Ferroptosis: a potential target for the treatment of atherosclerosis, Acta Biochim. Biophys. Sin. 56 (2024) 331–344.
[10] C.M. Weyand, B.R. Younge, J.J. Goronzy, T cells in arteritis and atherosclerosis, Curr. Opin. Lipidol. 19 (2008) 469–477.
[11] M.A. Postow, R. Sidlow, M.D. Hellmann, Immune-related adverse events associated with immune checkpoint blockade, N. Engl. J. Med. 378 (2018) 158–168.
[12] Z.D. Drobni, R.M. Alvi, J. Taron, A. Zafar, S.P. Murphy, P.K. Rambarat, R.C. Mosarla, C. Lee, D.A. Zlotoff, V.K. Raghu, S.E. Hartmann, H.K. Gilman, J. Gong, L. Zubiri, R.J. Sullivan, K.L. Reynolds, T. Mayrhofer, L. Zhang, U. Hoffmann, T.G. Neilan, Association between immune checkpoint inhibitors with cardiovascular events and atherosclerotic plaque, Circulation 142 (2020) 2299–2311.
[13] K. Poels, M.M.T. van Leent, M.E. Reiche, P.J.H. Kusters, S. Huveneers, M.P.J. de Winther, W.J.M. Mulder, E. Lutgens, T.T.P. Seijkens, Antibody-mediated inhibition of CTLA4 aggravates atherosclerotic plaque inflammation and progression in hyperlipidemic mice, Cells 9 (2020).
[14] T. Matsumoto, N. Sasaki, T. Yamashita, T. Emoto, K. Kasahara, T. Mizoguchi, T. Hayashi, K. Yodoi, N. Kitano, T. Saito, T. Yamaguchi, K. Hirata, Overexpression of cytotoxic T-lymphocyte-associated antigen-4 prevents atherosclerosis in mice, Arterioscler. Thromb. Vasc. Biol. 36 (2016) 1141–1151.
[15] M.M. Ewing, J.C. Karper, S. Abdul, R.C. de Jong, H.A. Peters, M.R. de Vries, A. Redeker, J. Kuiper, R.E. Toes, R. Arens, J.W. Jukema, P.H. Quax, T-cell co-stimulation by CD28-CD80/86 and its negative regulator CTLA-4 strongly influence accelerated atherosclerosis development, Int. J. Cardiol. 168 (2013) 1965–1974.

[16] D.M. Fernandez, A.H. Rahman, N.F. Fernandez, A. Chudnovskiy, E.D. Amir, L. Amadori, N.S. Khan, C.K. Wong, R. Shamailova, C.A. Hill, Z. Wang, R. Remark, J. R. Li, C. Pina, C. Faries, A.J. Awad, N. Moss, J.L.M. Bjorkegren, S. Kim-Schulze, S. Gnjatic, A. Ma'ayan, J. Mocco, P. Faries, M. Merad, C. Giannarelli, Single-cell immune landscape of human atherosclerotic plaques, Nat. Med. 25 (2019) 1576–1588.
[17] R. Saigusa, H. Winkels, K. Ley, T cell subsets and functions in atherosclerosis, Nat. Rev. Cardiol. 17 (2020) 387–401.
[18] I. Voloshyna, M.J. Littlefield, A.B. Reiss, Atherosclerosis and interferon-gamma: new insights and therapeutic targets, Trends Cardiovasc. Med. 24 (2014) 45–51.
[19] G.K. Hansson, P. Libby, The immune response in atherosclerosis: a double-edged sword, Nat. Rev. Immunol. 6 (2006) 508–519.
[20] A. Daugherty, D.L. Rateri, T lymphocytes in atherosclerosis: the yin-yang of Th1 and Th2 influence on lesion formation, Circ. Res. 90 (2002) 1039–1040.
[21] Y. Shibata, H. Ohata, M. Yamashita, S. Tsuji, J.F. Bradfield, A. Nishiyama, R.A. Henriksen, Q.N. Myrvik, Immunologic response enhances atherosclerosis-type 1 helper T cell (Th1)-to-type 2 helper T cell (Th2) shift and calcified atherosclerosis in Bacillus Calmette-Guerin (BCG)-treated apolipoprotein E-knockout (apo E-/-) mice, Transl. Res. 149 (2007) 62–69.
[22] C.M. Lloyd, E.M. Hessel, Functions of T cells in asthma: more than just T(H)2 cells, Nat. Rev. Immunol. 10 (2010) 838–848.
[23] H. Methe, S. Brunner, D. Wiegand, M. Nabauer, J. Koglin, E.R. Edelman, Enhanced T-helper-1 lymphocyte activation patterns in acute coronary syndromes, J. Am. Coll. Cardiol. 45 (2005) 1939–1945.
[24] X. Cheng, Y.H. Liao, H. Ge, B. Li, J. Zhang, J. Yuan, M. Wang, Y. Liu, Z. Guo, J. Chen, J. Zhang, L. Zhang, TH1/TH2 functional imbalance after acute myocardial infarction: coronary arterial inflammation or myocardial inflammation, J. Clin. Immunol. 25 (2005) 246–253.
[25] H. Yu, L. Lin, Z. Zhang, H. Zhang, H. Hu, Targeting NF-kappaB pathway for the therapy of diseases: mechanism and clinical study, Signal Transduct. Targeted Ther. 5 (2020) 209.
[26] B. Pamukcu, G.Y. Lip, E. Shantsila, The nuclear factor–kappa B pathway in atherosclerosis: a potential therapeutic target for atherothrombotic vascular disease, Thromb. Res. 128 (2011) 117–123.
[27] B. Mallavia, C. Recio, A. Oguiza, G. Ortiz-Munoz, I. Lazaro, V. Lopez-Parra, O. Lopez-Franco, S. Schindler, R. Depping, J. Egido, C. Gomez-Guerrero, Peptide inhibitor of NF-kappaB translocation ameliorates experimental atherosclerosis, Am. J. Pathol. 182 (2013) 1910–1921.
[28] M.A. Aronica, A.L. Mora, D.B. Mitchell, P.W. Finn, J.E. Johnson, J.R. Sheller, M.R. Boothby, Preferential role for NF-kappa B/Rel signaling in the type 1 but not type 2 T cell-dependent immune response in vivo, J. Immunol. 163 (1999) 5116–5124.
[29] R.Q. Guo, J.Z. Peng, Y.M. Li, X.G. Li, Microwave ablation combined with anti-PD-1/CTLA-4 therapy induces an antitumor immune response to renal cell carcinoma in a murine model, Cell Cycle 22 (2023) 242–254.
[30] S.J. O'Day, M. Maio, V. Chiarion-Sileni, T.F. Gajewski, H. Pehamberger, I.N. Bondarenko, P. Queirolo, L. Lundgren, S. Mikhailov, L. Roman, C. Verschraegen, R. Humphrey, R. Ibrahim, V. de Pril, A. Hoos, J.D. Wolchok, Efficacy and safety of ipilimumab monotherapy in patients with pretreated advanced melanoma: a multicenter single-arm phase II study, Ann. Oncol. 21 (2010) 1712–1717.
[31] T.A. Triplett, K.C. Garrison, N. Marshall, M. Donkor, J. Blazeck, C. Lamb, A. Qerqez, J.D. Dekker, Y. Tanno, W.C. Lu, C.S. Karamitros, K. Ford, B. Tan, X. M. Zhang, K. McGovern, S. Coma, Y. Kumada, M.S. Yamany, E. Sentandreu, G. Fromm, S. Tiziani, T.H. Schreiber, M. Manfredi, L.I.R. Ehrlich, E. Stone, G. Georgiou, Reversal of indoleamine 2,3-dioxygenase-mediated cancer immune suppression by systemic kynurenine depletion with a therapeutic enzyme, Nat. Biotechnol. 36 (2018) 758–764.
[32] J. Zhao, H. Zhang, Y. Huang, H. Wang, S. Wang, C. Zhao, Y. Liang, N. Yang, Bay11-7082 attenuates murine lupus nephritis via inhibiting NLRP3 inflammasome and NF-kappaB activation, Int. Immunopharm. 17 (2013) 116–122.
[33] M.M. Wu, J. Lou, B.L. Song, Y.F. Gong, Y.C. Li, C.J. Yu, Q.S. Wang, T.X. Ma, K. Ma, H.C. Hartzell, D.D. Duan, D. Zhao, Z.R. Zhang, Hypoxia augments the calcium-activated chloride current carried by anoctamin-1 in cardiac vascular endothelial cells of neonatal mice, Br. J. Pharmacol. 171 (2014) 3680–3692.
[34] W.L. Cheng, P.X. Wang, T. Wang, Y. Zhang, C. Du, H. Li, Y. Ji, Regulator of G-protein signalling 5 protects against atherosclerosis in apolipoprotein E-deficient mice, Br. J. Pharmacol. 172 (2015) 5676–5689.
[35] J. Zhu, B. Liu, Z. Wang, D. Wang, H. Ni, L. Zhang, Y. Wang, Exosomes from nicotine-stimulated macrophages accelerate atherosclerosis through miR-21-3p/PTEN-mediated VSMC migration and proliferation, Theranostics 9 (2019) 6901–6919.
[36] C. Liang, D. Zhu, W. Xia, Z. Hong, Q.S. Wang, Y. Sun, Y.C. Yang, S.Q. Han, L.L. Tang, J. Lou, M.M. Wu, Z.R. Zhang, Inhibition of YAP by lenvatinib in endothelial cells increases blood pressure through ferroptosis, Biochim. Biophys. Acta, Mol. Basis Dis. 1869 (2023) 166586.
[37] M.M. Wu, Y.C. Yang, Y.X. Cai, S. Jiang, H. Xiao, C. Miao, X.Y. Jin, Y. Sun, X. Bi, Z. Hong, D. Zhu, M. Yu, J.J. Mao, C.J. Yu, C. Liang, L.L. Tang, Q.S. Wang, Q. Shao, Q.H. Jiang, Z.W. Pan, Z.R. Zhang, Anti-CTLA-4 m2a antibody exacerbates cardiac injury in experimental autoimmune myocarditis mice by promoting ccl5-neutrophil infiltration, Adv. Sci. (2024) e2400486.
[38] X. Zhao, J. Tian, Y. Liu, Z. Ye, M. Xu, R. Huang, X. Song, TLR4-Myd88 pathway upregulated caveolin-1 expression contributes to coronary artery spasm, Vasc. Pharmacol. 142 (2022) 106947.
[39] J. Napetschnig, H. Wu, Molecular basis of NF-kappaB signaling, Annu. Rev. Biophys. 42 (2013) 443–468.
[40] C.J. Yu, C. Liang, Y.X. Li, Q.Q. Hu, W.W. Zheng, N. Niu, X. Yang, Z.R. Wang, X.D. Yu, B.L. Zhang, B.L. Song, Z.R. Zhang, ZNF307 (zinc finger protein 307) acts as a negative regulator of pressure overload-induced cardiac hypertrophy, Hypertension 69 (2017) 615–624.
[41] S. Strickson, D.G. Campbell, C.H. Emmerich, A. Knebel, L. Plater, M.S. Ritorto, N. Shpiro, P. Cohen, The anti-inflammatory drug BAY 11-7082 suppresses the MyD88-dependent signalling network by targeting the ubiquitin system, Biochem. J. 451 (2013) 427–437.
[42] Y. Wang, W. Sun, B. Du, X. Miao, Y. Bai, Y. Xin, Y. Tan, W. Cui, B. Liu, T. Cui, P.N. Epstein, Y. Fu, L. Cai, Therapeutic effect of MG-132 on diabetic cardiomyopathy is associated with its suppression of proteasomal activities: roles of Nrf 2 and NF-kappaB, Am. J. Physiol. Heart Circ. Physiol. 304 (2013) H567–H578.
[43] M. Roche-Molina, D. Sanz-Rosa, F.M. Cruz, J. Garcia-Prieto, S. Lopez, R. Abia, F.J. Muriana, V. Fuster, B. Ibanez, J.A. Bernal, Induction of sustained hypercholesterolemia by single adeno-associated virus-mediated gene transfer of mutant hPCSK9, Arterioscler. Thromb. Vasc. Biol. 35 (2015) 50–59.
[44] A. Gistera, D.F.J. Ketelhuth, S.G. Malin, G.K. Hansson, Animal models of atherosclerosis-supportive notes and tricks of the trade, Circ. Res. 130 (2022) 1869–1887.
[45] H. Bakhshi, S.A. Michelhaugh, S.A. Bruce, S.L. Seliger, X. Qian, B. Ambale Venkatesh, V. Varadarajan, P. Bagchi, J.A.C. Lima, C. deFilippi, Association between proteomic biomarkers and myocardial fibrosis measured by MRI: the multi-ethnic study of atherosclerosis, EBioMedicine 90 (2023) 104490.
[46] J. Wang, Y. Zhang, X. Feng, M. Du, S. Li, X. Chang, P. Liu, Tanshinone IIA alleviates atherosclerosis in LDLR(-/-) mice by regulating efferocytosis of macrophages, Front. Pharmacol. 14 (2023) 1233709.
[47] L. Chen, H. Chen, S. Guo, Z. Chen, H. Yang, Y. Liu, X. Chen, X. Chen, T. Du, X. Long, J. Zhao, M. Guo, T. Lao, D. Huang, L. Wang, J. Chen, C. Liu, Psoriasis comorbid with atherosclerosis meets in lipid metabolism, Front. Pharmacol. 14 (2023) 1308965.
[48] C. Blumm, G.A. Bonaterra, H. Schwarzbach, L.E. Eiden, E. Weihe, R. Kinscherf, PAC1 deficiency reduces chondrogenesis in atherosclerotic lesions of hypercholesterolemic ApoE-deficient mice, BMC Cardiovasc. Disord. 23 (2023) 566.
[49] K. Ma, S. Lv, B. Liu, Z. Liu, Y. Luo, W. Kong, Q. Xu, J. Feng, X. Wang, CTLA4-IgG ameliorates homocysteine-accelerated atherosclerosis by inhibiting T-cell overactivation in apoE(-/-) mice, Cardiovasc. Res. 97 (2013) 349–359.
[50] Z. Li, D. Ma, Y. Wang, S. Wu, L. Wang, Y. Jiang, Y. Zhang, X. Li, Astragali radix-coptis rhizoma herb pair attenuates atherosclerosis in ApoE-/- mice by regulating the M1/M2 and Th1/Th2 immune balance and activating the STAT6 signaling pathway, Evid Based Complement Alternat Med 2022 (2022) 7421265.
[51] E. Fiegle, D. Doleschel, S. Koletnik, A. Rix, R. Weiskirchen, E. Borkham-Kamphorst, F. Kiessling, W. Lederle, Dual CTLA-4 and PD-L1 blockade inhibits tumor growth and liver metastasis in a highly aggressive orthotopic mouse model of colon cancer, Neoplasia 21 (2019) 932–944.
[52] D. Schubert, C. Bode, R. Kenefeck, T.Z. Hou, J.B. Wing, A. Kennedy, A. Bulashevska, B.S. Petersen, A.A. Schaffer, B.A. Gruning, S. Unger, N. Frede, U. Baumann, T. Witte, R.E. Schmidt, G. Dueckers, T. Niehues, S. Seneviratne, M. Kanariou, C. Speckmann, S. Ehl, A. Rensing-Ehl, K. Warnatz, M. Rakhmanov, R. Thimme, P. Hasselblatt, F. Emmerich, T. Cathomen, R. Backofen, P. Fisch, M. Seidl, A. May, A. Schmitt-Graeff, S. Ikemizu, U. Salzer, A. Franke, S. Sakaguchi, L.S. K. Walker, D.M. Sansom, B. Grimbacher, Autosomal dominant immune dysregulation syndrome in humans with CTLA4 mutations, Nat. Med. 20 (2014) 1410–1416.

[53] H.S. Kuehn, W. Ouyang, B. Lo, E.K. Deenick, J.E. Niemela, D.T. Avery, J.N. Schickel, D.Q. Tran, J. Stoddard, Y. Zhang, D.M. Frucht, B. Dumitriu, P. Scheinberg, L.R. Folio, C.A. Frein, S. Price, C. Koh, T. Heller, C.M. Seroogy, A. Huttenlocher, V.K. Rao, H.C. Su, D. Kleiner, L.D. Notarangelo, Y. Rampertaap, K.N. Olivier, J. McElwee, J. Hughes, S. Pittaluga, J.B. Oliveira, E. Meffre, T.A. Fleisher, S.M. Holland, M.J. Lenardo, S.G. Tangye, G. Uzel, Immune dysregulation in human subjects with heterozygous germline mutations in CTLA4, Science 345 (2014) 1623–1627.
[54] Y. Hao, B. Miraghazadeh, R. Chand, A.R. Davies, C. Cardinez, K. Kwong, M.B. Downes, R.A. Sweet, P.F. Canete, L.J. D'Orsogna, D.A. Fulcher, S. Choo, D. Yip, G. Peters, S. Yip, M.J. Witney, M. Nekrasov, Z.P. Feng, D.C. Tscharke, C.G. Vinuesa, M.C. Cook, CTLA4 protects against maladaptive cytotoxicity during the differentiation of effector and follicular CD4(+) T cells, Cell. Mol. Immunol. 20 (2023) 777–793.
[55] E. Laurat, B. Poirier, E. Tupin, G. Caligiuri, G.K. Hansson, J. Bariety, A. Nicoletti, In vivo downregulation of T helper cell 1 immune responses reduces atherogenesis in apolipoprotein E-knockout mice, Circulation 104 (2001) 197–202.
[56] S. Eshghjoo, D.M. Kim, A. Jayaraman, Y. Sun, R.C. Alaniz, Macrophage polarization in atherosclerosis, Genes 13 (2022).
[57] C. Scheidereit, IkappaB kinase complexes: gateways to NF-kappaB activation and transcription, Oncogene 25 (2006) 6685–6705.
[58] N.D. Perkins, Integrating cell-signalling pathways with NF-kappaB and IKK function, Nat. Rev. Mol. Cell Biol. 8 (2007) 49–62.
[59] I. Pateras, C. Giaginis, C. Tsigris, E. Patsouris, S. Theocharis, NF-kappaB signaling at the crossroads of inflammation and atherogenesis: searching for new therapeutic links, Expert Opin. Ther. Targets 18 (2014) 1089–1101.
[60] H. Oh, S. Ghosh, NF-kappaB: roles and regulation in different CD4(+) T-cell subsets, Immunol. Rev. 252 (2013) 41–51.
[61] M.H. Park, J.T. Hong, Roles of NF-kappaB in cancer and inflammatory diseases and their therapeutic approaches, Cells 5 (2016).
[62] J.H. Fraser, M. Rincon, K.D. McCoy, G. Le Gros, CTLA4 ligation attenuates AP-1, NFAT and NF-kappaB activity in activated T cells, Eur. J. Immunol. 29 (1999) 838–844.
[63] Y. Zhang, B. Yang, J. Zhao, X. Li, L. Zhang, Z. Zhai, Proteasome inhibitor carbobenzoxy-L-leucyl-L-leucyl-L-leucinal (MG132) enhances therapeutic effect of paclitaxel on breast cancer by inhibiting nuclear factor (NF)-kappaB signaling, Med. Sci. Mon. Int. Med. J. Exp. Clin. Res. 24 (2018) 294–304.
[64] L. Chen, Y. Ruan, X. Wang, L. Min, Z. Shen, Y. Sun, X. Qin, BAY 11-7082, a nuclear factor-kappaB inhibitor, induces apoptosis and S phase arrest in gastric cancer cells, J. Gastroenterol. 49 (2014) 864–874.